Journal of Neurochemistry

WILEY | ISN International Society for Neurochemistry

ORIGINAL ARTICLE OPEN ACCESS

SPECIAL ISSUE Brain Organoids

CASPR2 Autoimmune Antibodies Induce Neuronal Hyperactivity in Human Brain Organoids

Ana Rafaela Oliveira[1,2,3] | Giuseppe Cammarata[1,4] | Catarina Seabra[1,3] | Ana Maria Cardoso[1,3] | Henrique J. Santos[1] | Joana Guedes[1,3] | Diana Sequeira[1,5] | João Miguel Marques Santos[5] | Guiomar Oliveira[6,7,8] | Ana Luísa Cardoso[1,3] | Dominique Fernandes[1,3] | Maria Isabel Leite[9,10] | Ester Coutinho[1,3,11] | Ana Luísa Carvalho[1,12] | Lino Ferreira[1,13] | João Peça[1,12]

[1]CNC-Center for Neuroscience and Cell Biology, University of Coimbra, Coimbra, Portugal | [2]MIT-Portugal PhD Program, NOVA School of Science and Technology, NOVA University Lisbon, Lisbon, Portugal | [3]Institute for Interdisciplinary Research (IIIUC), University of Coimbra, Coimbra, Portugal | [4]Doctoral Programme in Experimental Biology and Biomedicine (PDBEB), University of Coimbra, Coimbra, Portugal | [5]Faculty of Medicine, Institute of Endodontics, University of Coimbra, Coimbra, Portugal | [6]Child Developmental Centre and Centro de Investigação e Formação Clínica, Hospital Pediátrico, Centro Hospitalar e Universitário de Coimbra, Coimbra, Portugal | [7]Faculty of Medicine, University Clinic of Pediatrics, University of Coimbra, Coimbra, Portugal | [8]Clinical Academic Center of Coimbra (CACC), Coimbra, Portugal | [9]Oxford Autoimmune Neurology Group, Nuffield Department of Clinical Neurosciences, University of Oxford, Oxford, UK | [10]Department of Neurology, John Radcliffe Hospital, Oxford University Hospitals, Oxford, UK | [11]Faculty of Medicine, Universidade Católica Portuguesa, Lisbon, Portugal | [12]Department of Life Sciences, Faculty of Science and Technology, University of Coimbra, Coimbra, Portugal | [13]Faculty of Medicine, University of Coimbra, Coimbra, Portugal

Correspondence: João Peça (jpeca@cnc.uc.pt)

Received: 19 August 2025 | **Revised:** 14 December 2025 | **Accepted:** 3 February 2026

Keywords: autism | brain organoids | CASPR2 | electrophysiology | hyperexcitability | maternal autoantibodies | neurodevelopment

ABSTRACT

Gestational transfer of brain-reactive antibodies is a risk factor for neurodevelopmental disorders. Contactin-associated protein-like 2 (CASPR2) is a known target for pathogenic maternal autoantibodies which have been proposed to interfere with fetal neurodevelopment. However, the impact of CASPR2 antibodies on human brain development remains largely unknown. Here, to better understand the neurophysiological changes that occur in the presence of these pathogenic autoantibodies, we cultured unguided human neural organoids for a period of 6-months in media containing anti-CASPR2 antibodies. We then performed neurophysiological characterization via whole-cell patch-clamp and calcium imaging in acute organoid slices. Our results reveal that CASPR2 antibody exposure increased spontaneous synaptic activity, enhanced the maximal frequency of action potential firing and of spontaneous network activity. These findings are consistent with a state of neuronal hyperexcitability, a phenotype which is observed in several models of neurodevelopmental disorders. Mechanistically, the alterations observed in action potential waveform are in accordance with a role for CASPR2 in the regulation of voltage-gated potassium channels and a pathological role for CASPR2 autoantibodies in driving neuronal hyperexcitability.

Abbreviations: AP, action potential; ASD, Autism Spectrum Disorder; CASPR2, contactin-associated protein-like 2; CASPR2-Ab, CASPR2 antibodies; Cm, membrane capacitance; CNTNAP2, contactin-associated protein-like 2; CTR, control; DLX2, distal-less homeobox 2; E/I, excitation/inhibition ratio; fAHP, action potential fast-afterhyperpolarization; GABA, gamma-aminobutyric acid; GAD1, glutamate decarboxylase 1; GAD67, glutamate decarboxylase 67; GFAP, glial fibrillary acidic protein; HEK, Human Embryonic Kidney; hiPSCs, human induced pluripotent stem cells; IgG, immunoglobulin G; Irh, rheobase current; KO, knockout; Kv, voltage-gated potassium channels; MAG, myelin-associated glycoprotein; MAL, myelin and lymphocyte protein; MAP 2, microtubule-associated protein 2; MOG, myelin oligodendrocyte glycoprotein; mRNA, messenger ribonucleic acid; NaV, voltage-gated sodium channels; NESTIN, neuroectodermal stem cell protein; NEUN, neuronal nuclei (RBFOX3); OLIG2, oligodendrocyte transcription factor 2; PAX6, paired box protein Pax-6; PVALB, parvalbumin; Ra, access resistance; RRID, Research Resource Identifier; Rm, membrane resistance; RMP, resting membrane potential; SATB2, special AT-rich sequence-binding protein 2; sEPSCs, spontaneous excitatory postsynaptic currents; SLC17A7, solute carrier family 17 member 7; SOX2, SRY-box transcription factor 2; TBR1, T-box, brain 1; TH, tyrosine hydroxylase; VGKCs, voltage-gated potassium channels; VGLUT, vesicular glutamate transporter; Vth, threshold potential; β-III tubulin, Class III β-tubulin (TUJ1).

1 | Introduction

Contactin-associated protein-like 2 (CASPR2) is encoded by the *CNTNAP2* gene, a member of the neurexin superfamily of transmembrane proteins that mediate cell–cell interactions (Poliak et al. 1999). This protein forms a complex with Contactin-2/TAG-1 to stabilize voltage-gated potassium channels (VGKCs) at the juxtaparanodal regions of myelinated axons (Poliak et al. 2003; Pinatel et al. 2017). Consistent with VGKCs providing crucial regulation over neuronal excitability (Bertil Hille 1992), immune or genetic perturbations of CASPR2 result in Kv1 channel mislocalization and dysfunction, ultimately leading to enhanced neuronal excitability in rodent models (Dawes et al. 2018; Joubert et al. 2022).

Beyond its primary role in regulating VGKCs, CASPR2 is also involved in additional neural roles. As evidenced in the *Cntnap2* knockout (KO) mice, CASPR2 modulates inhibitory tone in neural circuits, leading to decreased inhibition in the CA1 region of the hippocampus, hyperactivity and seizures (Jurgensen and Castillo 2015). These mice also show a reduced number of GABAergic interneurons, including parvalbumin-positive ($PVALB^+$) cortical interneurons in the somatosensory cortex (Peñagarikano et al. 2011; Vogt et al. 2018). Furthermore, CASPR2 influences dendritic arborization, spine development and stabilization, thereby impacting neuronal network activity (Anderson et al. 2012; Gdalyahu et al. 2015) and glutamatergic synaptic activity (Fernandes et al. 2019; Varea et al. 2015).

Clinical relevance of CASPR2 is increasingly recognized as the result both from genetic mutations and autoimmune pathology. Mutations in *CNTNAP2* are linked to a spectrum of neurodevelopmental and neuropsychiatric disorders (Rodenas-Cuadrado et al. 2014). Notably, rare homozygous loss-of-function mutations and risk variants contribute to forms of autism characterized by intellectual disability, language regression, seizures, and cortical dysplasia (Strauss et al. 2006; Alarcón et al. 2008). Beyond these genetic associations, CASPR2 has also been established as an antigen in autoimmune synaptic encephalitis (Irani et al. 2010; Lancaster et al. 2011), a rare central nervous system syndrome characterized by memory disorders, temporal lobe seizures, and frontal lobe impairments. Building on this understanding of antibody-mediated pathology, more recent investigations have revealed that CASPR2 antibodies (CASPR2-Ab) can also contribute to neurodevelopmental disorders through gestational transfer from mother to fetus (Brimberg et al. 2016; Coutinho, Jacobson, et al. 2017; Bagnall-Moreau et al. 2020). Together, these findings highlight *CNTNAP2* as a gene of major importance for understanding the molecular underpinnings of Autism Spectrum Disorder (ASD) and support a model in which CASPR2 dysfunction impairs critical neurodevelopmental processes essential for higher-order cognition and behavior.

However, despite collective findings on potential roles for CASPR2, the specific neurobiological relevance through which maternally-derived CASPR2-Ab leads to neuronal dysfunction during early human neurodevelopment remains to be characterized. Therefore, and to directly address this question, we characterized human organoids after long-term exposure to plasma containing CASPR2-Ab. Using acute slices and whole-cell patch-clamp, we found increased levels of synaptic activity in neurons from organoids incubated with CASPR2-Ab. Additionally, calcium imaging revealed increased levels of spontaneous activity. Under current clamp recordings, action potential (AP) waveform analysis disclosed an increase in maximal firing frequency and a shallower action potential fast-afterhyperpolarization (fAHP). This latter alteration is congruent with the phenotype of enhanced neuronal hyperexcitability, supports the canonical role of CASPR2 in regulating VGKCs, and suggests a novel contribution of CASPR2 to the control of network activity during human neurodevelopment.

2 | Methods

2.1 | Human Samples

Plasma exchange samples obtained from a 72-year-old male patient with CASPR2 autoimmune encephalitis, experiencing periods of disease exacerbation, were collected at the John Radcliffe Hospital, Oxford University. The patient presented high levels of CASPR2 autoantibodies, developed Morvan's syndrome, progressive neuropathic pain, episodes of lack of perception with goosebumps, and memory complaints (short- and long-term memory, including word-finding difficulties), with no indication of paraneoplastic causes. Control plasma was collected from healthy individuals in a protocol approved by the Ethical Committee of Centro Hospitalar Universitário de Coimbra (Ethics approval Ref. CHUC-065-18). Procedures followed the guidelines of the Declaration of Helsinki and written informed consent was obtained from the patient and healthy controls.

2.2 | Human Induced Pluripotent Stem Cells (hiPSCs) Culture

Data throughout the manuscript derive from at least two independent differentiation experiments, each initiated from a separate iPSC thaw and embryoid body formation. Two human iPSC lines were used in this study, NCBL1.c5 (RRID:CVCL_C0P1) and 31f-r1 (RRID:CVCL_1E85), with their use varying by experimental modality. For the qPCR analyses and the Ca^{2+} imaging experiments, both iPSC lines were employed, and comparable results were obtained from both, supporting the reproducibility of the observed phenotypes across distinct genetic backgrounds. The whole-cell recordings were performed exclusively using the 31f-r1 line.

The NCBL1.c5 hiPSCs were generated from human dermal fibroblasts of a healthy donor through episomal nucleofection of Yamanaka factors (Oct3/4, Sox2, Klf4, and L-Myc), as described in (Oliveira et al. 2022) and based on the method of (Howden et al. 2015). The 31f-r1 hiPSC line (iLB-C-31f-r1), kindly provided by Prof. Dr. Oliver Brüstle (University of Bonn), was reprogrammed from human dermal fibroblasts using lentiviral delivery of Oct3/4, Sox2, c-Myc, and Klf4.

Both lines were maintained under identical culture conditions: hiPSCs were grown on Matrigel-coated plates (Corning Matrigel; Catalog #354277) in mTeSR Plus medium (STEMCELL Technologies; Catalog #05825) supplemented with 1% Penicillin/Streptomycin (Gibco), at 37°C and 5% CO_2, and passaged every

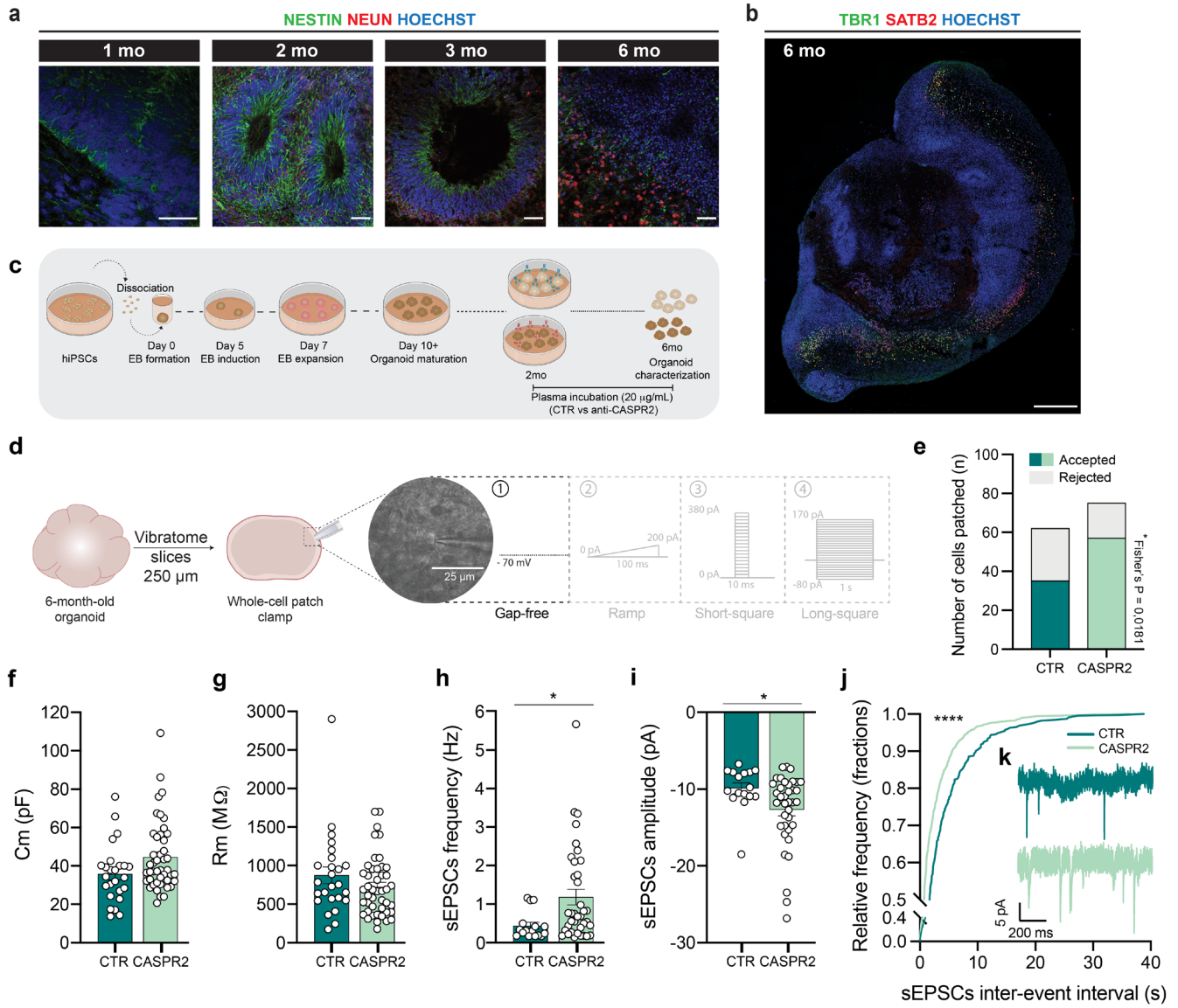

FIGURE 1 | Increased synaptic activity in human brain organoids exposed to CASPR2-Ab. (a, b) Representative images of unguided neural organoids maturation collected at 1, 2, 3 and 6 months of in vitro development, using immunohistochemistry directed at Nestin and NeuN (a); and TBR1 and SATB2 (b). Scale bars: 50 µm (a) or 500 µm (b). (c) Schematic representation of the experimental procedure and incubation using 20 µg/mL of control (CTR) or CASPR2-Ab rich plasma, from Month 2 to 6 of organoid maturation, with twice weekly changes of medium and addition of fresh plasma. (d) Schematic representation of the recording protocols used for whole-cell recording. (e) Proportion of cells surviving inclusion criteria in organoids treated with CTR or CASPR2-Ab (see text and methods section for details). (f, g) Cell capacitance (f) and membrane resistance (g) were not significantly different between treatments. (h–k) sEPSCs showed elevated frequency (h) and amplitude (i), with inter-event intervals significantly shifted across the entire distribution (j, k). CTR $n = 16–25$ cells, 7 organoids; CASPR2 $n = 37–45$ cells, 7 organoids. Each dot represents one cell. Data is presented as a cumulative frequency plot in (j), all other plots are presented as mean ± SEM. Statistical tests: Fisher's exact test (e), two-tailed Mann–Whitney test (f–i), Kolmogorov–Smirnov test (j); significance: $^{*}p < 0.05$, $^{****}p < 0.0001$.

3–5 days using ReLeSR (STEMCELL Technologies; Catalog #05872) for gentle dissociation. Cells were routinely tested for mycoplasma contamination and maintained in culture for a maximum of 35 passages.

2.3 | Generation of Human Unguided Neural Organoids and Plasma Incubation

Unguided neural organoids were generated based on the protocol published by Lancaster et al. (Lancaster et al. 2013; Lancaster and Knoblich 2014), with the modifications presented in the STEMdiff Cerebral Organoid Kit (Stem Cell Technologies; Catalog #08570), as illustrated in Figure 1. In brief, hiPSCs colonies were dissociated using Accutase (Stem Cell Technologies; Catalog #07920) and 9000 cells per well were plated on a 96-well cell suspension plate (Greiner Bio-One) in EB Formation Medium with 10 µM of the ROCK inhibitor Y-27632 (Stem Cell Technologies; Catalog #72307). Embryoid bodies were fed on Day 2 and Day 4 with EB Formation Medium and transferred to 24-well cell suspension plates (Greiner Bio-One) in Induction Medium, on Day 5. On Day 7, EBs were embedded on droplets

of cold Matrigel (Corning Matrigel; Catalog #354277) on a sheet of Parafilm. The droplets were allowed to polymerize at 37°C for 30 min and were subsequently removed from the Parafilm and grown in Expansion Medium for 3 days in ultra-low-attachment 6-well plates (Corning). Afterwards, the EB droplets were kept in suspension in Maturation Medium and placed on an orbital shaker at 65 rpm. Organoids were maintained exclusively in Maturation Medium for up to 6 months, with exposure to CASPR2 encephalitis patient or healthy control plasma (20 μg/mL) from 2 months of differentiation onwards. The media was changed every 3–4 days with addition of fresh plasma.

2.4 | Immunohistochemistry

Organoids were collected at different ages, from 1 to 6 months of differentiation. Upon collection, they were fixed in 4% PFA for 90 min and then transferred to a solution of 30% sucrose in PBS 1× for cryoprotection. Subsequently, they were transferred into OCT embedding matrix (VWR), snap-frozen on dry ice and stored at −80°C until further use for immunohistochemistry experiments.

Using a cryostat, 20 μm thick sections were obtained and collected directly into adhesive Superfrost Plus slides (Thermo Scientific Menzel). Cryosections were washed twice with PBS 1× and permeabilized with 0.5% Triton X-100 in PBS 1× for 15 min at room temperature (RT). Sections were then blocked in 3% BSA in PBS 1× for 1 h at RT and incubated with primary antibodies diluted in 3% BSA in PBS 1× overnight at 4°C. The next day, sections were washed twice with PBS 1× and incubated for 2 h at RT with the secondary antibodies diluted 1:200 in 3% BSA in PBS 1×. Nuclei were stained with Hoechst 33342 (1 μg/mL) for 5 min in the dark. Sections were washed twice in PBS 1× and mounted for microscopy using Dako Fluorescent Mounting Medium (Dako). Images were acquired using a Zeiss Confocal LSM 710 microscope with a 20× air or 60× oil objective and processed using Zen Software (Zeiss). The antibodies used in this work are described in Table S1. Combinations of antibodies used in tandem are described in the figure legends.

2.5 | Real Time Quantitative PCR (qRT-PCR)

RNA was extracted from frozen organoids from 1 to 6 months of differentiation using the NucleoSpin RNA Isolation Kit (Macherey-Nagel; Catalog #740955.50), according to the manufacturer's recommendations for cultured cells. Complementary DNA (cDNA) was synthesized from 150 ng and 800 ng of total extracted RNA using the NZY First-Strand cDNA Synthesis Kit (Nzytech; Catalog #MB12501), following the instructions from the supplier. The synthesized cDNA was further diluted 20 times with RNase-free water and stored at −20°C until required for quantitative PCR analysis. qRT-PCR was accomplished in a StepOnePlus thermocycler (Applied Biosystems) using 96-well low-profile microtitre plates (Nerbe Plus) and employing the NZYSpeedy qPCR Green Master Mix 2× (Nzytech; Catalog #MB22402) for mRNA quantification. Relative mRNA levels were determined following the Pfaffl method (Pfaffl 2001), taking into consideration the different amplification efficiencies of each primer, obtained from a standard curve of serial sample dilutions, determined according to the formula $E = 10^{[-1/\text{slope}]}$. Values were normalized to the average expression of *GAPDH* and *HPRT*. PCR primer sequences used are presented in Table S2.

2.6 | Slice Preparation for Whole-Cell Patch Clamp and Ca^{2+} Imaging

Organoid slices were obtained as previously described in (Paşca et al. 2015) with some modifications. The organoids were first removed from Maturation Medium and placed into a mold with a 3% low-melting agarose solution prepared in PBS 1×. After gelification, the agarose containing the organoid was quickly removed and glued to a vibratome support filled with ice-cold oxygenated (95%:5% O_2:CO_2 mix) N-Methyl-D-Glucamine-enriched artificial cerebrospinal fluid (NMDG-aCSF) containing 99.69 mM NMDG, 2.55 mM KCl, 30 mM $NaHCO_3$, 1.23 mM $NaH_2PO_4.H_2O$, 20 mM HEPES, 25 mM glucose, 1.97 mM thiourea, 4.99 mM Na-ascorbate, 2.99 mM Na-pyruvate, 10 mM $MgSO_4$ and 0.5 mM $CaCl_2$. Slices of 250 μm were obtained using a vibratome (Leica VT1200s, Leica Microsystems, USA) and immediately recovered in a bath at 32°C for 8 min in NMDG-aCSF. Slices were then moved to a holding chamber that contained oxygenated aCSF at 25°C (127.48 mM NaCl, 2.55 mM KCl, 24.04 mM $NaHCO_3$, 1.23 mM $NaH_2PO_4.2H_2O$, 12.49 mM glucose, 2 mM $MgSO_4$ and 2 mM $CaCl_2$). Slices were maintained in aCSF for at least 1 h before recording. The osmolarity of NMDG-aCSF and aCSF was adjusted to 300–310 mOsm and the pH was adjusted to 7.3–7.4 with HCl.

2.7 | Whole-Cell Patch Clamp Recordings

Whole-cell patch clamp recordings were registered in a recording chamber perfused with aCSF (2–3 mL/min) at 25°C. The cells were visualized with an Axio Examiner.D1 microscope (Carl Zeiss) equipped with a Q-capture Pro7 camera (Teledyne), and putative pyramidal-shaped neurons near the surface of organoids were identified under infrared-differential interference contrast visualization with a 40× objective. Cells were patched with borosilicate glass recording electrodes (3–7 MΩ; Science Products) filled with an internal solution of potassium-gluconate (K-int) containing: 145 mM K-gluconate, 10 mM HEPES, 1 mM EGTA, 2 mM ATP-magnesium salt, 0.3 mM GTP-sodium salt, and 2 mM $MgCl_2.6H_20$, pH adjusted to 7.36 with NaOH (298–300 mOsm). The recorded neurons were voltage-clamped at −70 mV to record sEPSCs, and the recording was performed for 3 min (gap-free protocol). The resting membrane potential (RMP) and action potentials (APs) parameters were estimated under current-clamp mode. The RMP and the neuronal excitability were obtained by stepped current injection (1000 ms duration, 10 pA stepwise from −80 pA to +170 pA—Long-square protocol). The kinetics of the APs were acquired by stepped current injection (10 ms duration, 20 pA stepwise from 0 pA to +380 pA—Short-square protocol). Criteria for acceptance of cells was determined as an initial access resistance under 25 MΩ, which did not increase more than 30% during the recording, RMP ≤ −40 mV, and cells firing activity upon current injection. Recordings were filtered at 2 kHz and digitized at 20 kHz. All electrophysiology data were acquired with a Multiclamp 700B amplifier and Digidata 1550A (Molecular Devices). Voltage clamp data were analyzed using Clampfit software (v.10.7, Molecular

Devices), and current clamp data were analyzed using Easy Electrophysiology Software (v.2.4.0). All electrophysiological experiments were performed between weeks 25 and 28 of in vitro differentiation.

2.8 | Ca^{2+} Imaging Recordings

Slices were loaded with 4.5 μM Fluo-4 AM (acetoxymethyl ester) (Invitrogen; Catalog #F14201) in aCSF solution for 30 min in an incubator at 37°C, 5% CO_2. After 30 min, slices were washed with PBS 1× and mounted on an inverted fluorescence microscope (Zeiss Cell Observer Spinning Disk). Imaging was performed at 37°C and 5% CO_2 and the emission fluorescence was recorded at 506 nm by a highly sensitive electron multiplying camera (EM-CCD Evolve Delta). The time course of the experiments consisted of 200 ms of exposure for a total of 750 frames. Imaging processing, including background subtraction, frame alignment and bleach correction, was performed using ImageJ (Fiji). ROIs (regions of interest) corresponded to a single microdomain, which may correspond to subcellular regions or to clusters of cells depending on signal synchrony. ROI related activity was selected using the calcium imaging analyzer (CALIMA) software and the frequency of firing was calculated using Clampfit software (v.10.7, Molecular Devices).

2.9 | Data Collection and Statistical Analysis

Data analysis was performed by experimenters blind to treatment group. Raw data values are presented as individual scatter plots and averages represented as mean values ± SEM (standard error of the mean). Statistical analysis was calculated using unpaired two-tailed Student *t*-test, two-tailed Mann–Whitney test, repeated measures two-way ANOVA or Kolmogorov–Smirnov test. Before application of parametric tests, sample normality was tested using D'Agostino-Pearson test. Full statistical reports are presented in Table S3. Analysis was performed using the standard statistical software GraphPad Prism 8. Differences were considered statistically significant for p values < 0.05 ($^{*}p < 0.05$, $^{**}p < 0.01$, $^{****}p < 0.0001$). No formal outlier test was conducted. Sample size calculation was estimated based on prior experience (Oliveira et al. 2022; Martins et al. 2023; Guedes et al. 2023) and a priori sample size calculation was not performed.

3 | Results

3.1 | Neuronal Features of Human Neural Organoids Through 6 Months in Culture

Unguided neural organoids generated from hiPSCs were characterized for up to 6 months of in vitro maturation. We first tested for the expression of markers of neuronal progenitors, mature neurons, glia and of neuronal subtypes using immunohistochemistry and qRT-PCR from 1 to 6 months in vitro (Figure 1 and Figure S1). Mature neurons, positive for NEUN, appeared reliably after 3 months (Figure 1a), and TBR1 and SATB2 staining revealed early-born and late-born neurons, respectively, organized along a cortical-like layer in organoids grown for 6 months in vitro (Figure 1b). Additionally, we observed the expected variety of cell types, including astrocytes, that started to show intense labeling for GFAP after 3–6 months in culture (Figure S1b,h), and mRNA for oligodendrocyte precursors, which was observed at 6 months (Figure S1h). In 6-month-old organoids, we observed widespread labeling for the excitatory neuronal marker VGLUT, as well as sparse GAD67 labeling (inhibitory neurons) and tyrosine hydroxylase (TH)-positive staining (dopaminergic neurons) (Figure S1c,d).

During prolonged maturation, we observed a small decrease in the expression of neuronal progenitor genes (*SOX2* and *NESTIN*), followed by an increase in the early neuronal gene *β-III TUBULIN* (TUJ1). However, *MAP2* and *β-III TUBULIN* expression levels were highest in brain organoids with 3 months (Figure S1e). This may be associated with cell death at later ages (Tanaka et al. 2020) or, alternatively, due to skewed prevalence of certain cellular populations appearing only at later stages (e.g., astrocytes and oligodendrocytes). This dynamic change could, in bulk analysis, lead to a relative dilution of neuronal-specific mRNAs in later timepoints.

Additionally, we evaluated the expression of sodium- and potassium-voltage gated channels, as well as markers for excitatory and inhibitory neurons (Figure S1f,g). Again, we found a similar decrease in expression at later timepoints, coinciding with the increased expression of astrocyte and oligodendrocyte markers (Figure S1h). As previously reported (Renner et al. 2017), *GFAP* and *OLIG2* showed an increase in their expression over time, with little to no expression in the first months of differentiation (Figure S1h). Together, these results suggest that in our experimental conditions, the presence of neurons and glia—which are important for proper neuronal activity—converge at the timepoint of 5–6 months in culture. This indication matched pilot electrophysiology experiments performed to assess the competency of neurons to fire action potentials, which tended to occur reliably only beyond the 5-month maturation period (data not shown). Therefore, our data collection was directed towards organoids developing in culture until 6-months of age.

Due to the nature of our approach, we tested the binding specificity of plasma containing CASPR2-Ab to CASPR2 (Figure S2). For this assessment, and as previously reported (Coutinho, Menassa, et al. 2017; Fernandes et al. 2019), we showed that CASPR2-Ab in the plasma of an encephalitis patient binds to the surface of both rat cortical neurons and HEK cells overexpressing human CASPR2 (Figure S2). This same plasma did not show reactivity to HEK cells transfected with a control plasmid (Figure S2). Importantly, we also showed that control plasma (CTR) from a healthy individual did not react with cortical neurons, nor to CASPR2- nor CTR-transfected HEK cells (Figure S2) or to CNTNAP2 KO neurons, as previously reported (Fernandes et al. 2019). This indicates that control plasma does not contain antibodies against CASPR2 or other neuronal surface proteins. Additionally, due to the long-term incubations being performed, we also aimed to assess if antibodies present in the plasma would become depleted over time or remain active between media changes. For this experiment, we used conditioned media containing CTR or CASPR2 plasma (at an initial IgG concentration of 20 μg/mL), collected from the organoid cultures before a fresh media exchange

and performed. This conditioned media was then used to re-incubate HEK-transfected cells (Figure S3). In this experiment, we could still observe significant IgG staining in CASPR2-transfected cells after exposure to the conditioned media, suggesting CASPR2-Ab are not depleted from the medium during 3–4 days in culture, between media replenishment.

3.2 | CASPR2-Antibodies Do Not Alter Basic Neuronal Membrane Properties, but Modify Synaptic Connectivity

Brain organoids for characterization were exposed to CASPR2 or CTR plasma from Month 2 to 6 of differentiation, with twice weekly changes of medium containing fresh plasma (20 μg/mL) (Figure 1c). Considering the role of CASPR2 in regulating voltage-gated potassium channels, we sought to determine the effect of CASPR2-Ab on neuronal excitability during early brain development. For this, we performed whole-cell patch-clamp in neurons in acute organoid slices. Cells were included in the analysis based on the following criteria: (i) initial access resistance (Ra) < 25 MΩ; (ii) difference between the initial Ra and the final Ra < 30%; and (iii) resting membrane potential (RMP) ≤ −40 mV. From a total of 62 patched cells in CTR condition and 75 cells in CASPR2 condition (from 7 organoids in each condition), we retained 35 cells in the CTR condition and 57 cells in the CASPR2 condition ($p = 0.0181$, Fisher's Exact test; Figure 1e). The retained cells that met these criteria were subjected to a set of experimental protocols or further rejected if, for example, they failed to show the ability to fire action potentials or reach protocol specific criteria (e.g., 30 spontaneous synaptic events within a 3-min recording).

In terms of intrinsic neuronal membrane properties, capacitance ($Cm_{CTR} = 35.84 \pm 3.050$ pF, $n = 25$; $Cm_{CASPR2} = 44.60 \pm 2.723$ pF, $n = 45$; $p = 0.0575$) and membrane resistance ($Rm_{CTR} = 874.9 \pm 108.9$ MΩ, $n = 25$; $Rm_{CASPR2} = 725.5 \pm 57.01$ MΩ, $n = 45$; $p = 0.2231$) were not statistically different between conditions, however, there was a pronounced trend for larger capacitance in neurons from CASPR2-Ab organoids (Figure 1f,g). Next, we assessed spontaneous excitatory postsynaptic currents (sEPSCs) and observed an increase in amplitude ($sEPSCs_{CTR} = -9.886 \pm 0.6999$ pA, $n = 16$; $sEPSCs_{CASPR2} = -12.69 \pm 0.7845$ pA, $n = 37$; $p = 0.0203$) and frequency ($sEPSCs_{CTR} = 0.4400 \pm 0.08839$ Hz, $n = 16$; $sEPSCs_{CASPR2} = 1.182 \pm 0.2022$ Hz, $n = 37$; $p = 0.0118$) of events in neurons from CASPR2-Ab-exposed organoids (Figure 1h,i). Additionally, analysis of inter-event intervals revealed a significant shift in event distribution, as shown by the cumulative probability plots when considering all detected sEPSCs ($ISI_{CTR} = 3.5919 \pm 0.24237$ s, $n = 464$; $ISI_{CASPR2} = 2.1297 \pm 0.11082$ s, $n = 1073$; Kolmogorov–Smirnov $D = 0.1779$; $p < 0.0001$) (Figure 1j,k). These results suggest that exposure to CASPR2-Ab might impact network neuronal activity by enhancing both the number and strength of excitatory synapses.

3.3 | CASPR2 Antibodies Influence Action Potential Repolarization

Considering the role of CASPR2 in regulating voltage-gated potassium channels, we sought to determine the effect of CASPR2-Ab on AP kinetics during early brain development (Figure 2). First, we analyzed the number of cells that would discharge an AP under a ramp, short-square or long-square current injection protocol (Figure 2a,b). Neurons from CTR organoids appeared in similar proportion in terms of the capacity to fire AP when compared to those from the CASPR2-Ab condition (CTR = 25/35 vs. CASPR2 = 45/57; $p = 0.4563$, Fisher's Exact test; Figure 2b: top). However, CASPR2-Ab exposed neurons showed an increased probability of firing in both a short-square and long-square protocols (CTR = 60%, CASPR2 = 89%, $p = 0.0153$ Fisher's Exact test; Figure 2b: bottom). These data could suggest that in CASPR2-Ab treated organoids, neurons display more robust capability to respond to various depolarizing challenges.

We recorded the resting membrane potential (RMP), threshold potential, and rheobase from neurons in CTR and CASPR2-Ab treated organoids (Figure 2c–e). We found no major differences in RMP ($RMP_{CTR} = -57.40 \pm 1.688$ mV, $n = 25$; $RMP_{CASPR2} = -58.09 \pm 1.125$ mV, $n = 45$; $p = 0.6416$), suggesting that cells were significantly polarized, while resting, in either condition (Figure 2c). In the ramp test, the current necessary to elicit an action potential was also similar ($Irh_{CTR} = -35.38 \pm 4.062$ pA, $n = 22$; $Irh_{CASPR2} = 33.91 \pm 2.545$ pA, $n = 45$; $p = 0.9446$) (Figure 2d). From the latter, we could calculate the threshold potential, which was again not significantly altered ($Vth_{CTR} = -26.33 \pm 1.739$ mV, $n = 22$; $Vth_{CASPR2} = -29.59 \pm 1.111$ mV, $n = 45$; $p = 0.1141$) (Figure 2e).

Since CASPR2 is known to influence the clustering and function of VGKC, we analyzed the waveform of single action potentials induced in a short-square current injection protocol (Figure 2f,g). For this analysis, we determined different parameters, including AP peak voltage, peak amplitude, half-width, rise time, decay time, and fast-afterhyperpolarization (fAHP) amplitude and minimum fAHP voltage (Figure 2h–n). The action potential peak ($AP_{CTR} = 32.62 \pm 1.736$ mV, $n = 17$; $AP_{CASPR2} = 34.69 \pm 1.328$ mV, $n = 41$; $p = 0.2624$) and peak amplitude ($AP\Delta_{CTR} = 54.28 \pm 4.078$ mV, $n = 17$; $AP\Delta_{CASPR2} = 56.05 \pm 1.917$ mV, $n = 41$; $p = 0.8392$) were not significantly altered (Figure 2h,i). The kinetic parameters related to the AP waveform, including the half-width ($APw_{CTR} = 3.556 \pm 0.3454$ ms, $n = 17$; $APw_{CASPR2} = 3.094 \pm 0.2294$ ms, $n = 41$; $p = 0.1834$), rise time ($APtr_{CTR} = 0.9129 \pm 0.08286$ ms, $n = 17$; $APtr_{CASPR2} = 0.8356 \pm 0.03978$ ms, $n = 41$; $p = 0.7575$), or decay time ($AP\tau_{CTR} = 18.21 \pm 0.7440$ ms, $n = 17$; $AP\tau_{CASPR2} = 15.71 \pm 0.9400$ ms, $n = 41$; $p = 0.2084$) were also not significantly altered in neurons f both conditions (Figure 2j–l).

However, the fAHP amplitude ($fAHP_{CTR} = -37.28 \pm 2.108$ mV, $n = 17$; $fAHP_{CASPR2} = -31.97 \pm 1.361$ mV, $n = 41$; $p = 0.0391$) was decreased and the minimum voltage of fAHP was also less negative in CASPR2-Ab exposed organoids ($fAHPm_{CTR} = -57.45 \pm 2.118$ mV, $n = 17$; $fAHPm_{CASPR2} = -53.18 \pm 0.9776$ mV, $n = 41$; $p = 0.0406$) (Figure 2m,n). These data indicate there is a reduced depolarization shift in the CARPR2-Ab condition, which, considering the other largely intact parameters of the AP, suggests a specific alteration in the VGKCs involved in the spike hyperpolarizing phase, consistent with the physiological role of Kv1 channels (Storm 1988).

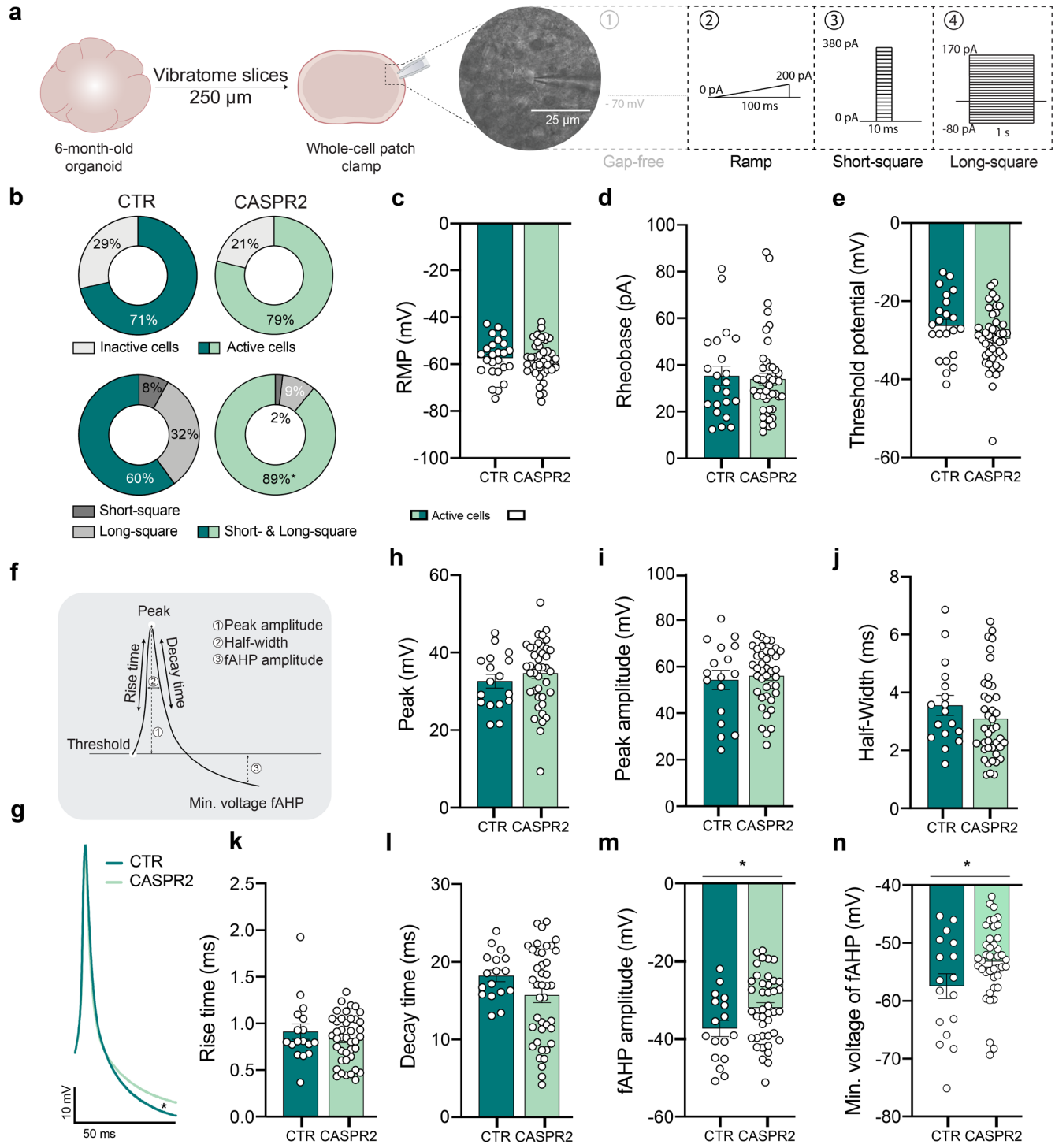

FIGURE 2 | Neurons from organoids incubated with CASPR2-Ab reveal alteration in action potential fast-afterhyperpolarization. (a) Whole-cell patch-clamp was performed in acute organoid slices of 250 µm and three different protocols were used: ramp, short- and long-square protocol. (b) CASPR2-exposed organoids showed a similar percentage of cells presenting neuronal activity (71% CTR vs. 79% CASPR2, $p = 0.4563$), but an increased frequency of neurons that respond to both short-square and long-square stimulation (60% CTR vs. 89% CASPR2; $p = 0.0155$). (c–e) Intrinsic neuronal properties: RMP—resting membrane potential (c), rheobase (d), and threshold potential (e) were not significantly altered between conditions. (f–n) Action potentials parameters in neurons from CTR and CASPR2-Ab condition did not show significant differences in AP peak voltage (h), peak amplitude (i), AP half-width (j), AP rise time (k) or decay time (l); however, the amplitude of the fast-afterhyperpolarization (fAHP) (m) was less negative in the CASPR2 condition, and the fAHP minimum voltage was also less depolarized (n). CTR $n = 25–35$ cells, 7 organoids; CASPR2 $n = 45–57$ cells, 7 organoids. Each dot represents one cell. Data is presented as mean ± SEM. Statistical tests: Fisher's exact test (b), two-tailed Mann–Whitney test (c–e and h–l) and two-tailed Student *t*-test (m, n); significance: $^*p < 0.05$.

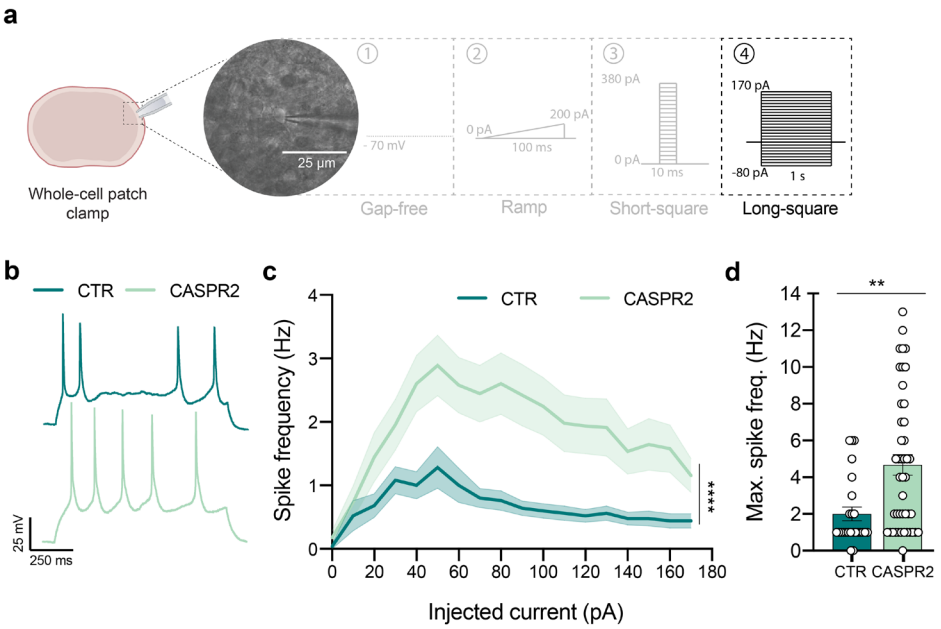

FIGURE 3 | Increased neuronal excitability in human neurons incubated with CASPR2-Ab. (a) A long-square stimulation protocol was used to assess neuronal excitability in 250 µm acute organoid slices. (b, c). Upon current injection, neurons in CASPR2-exposed organoids presented an increased frequency of action potential firing. (d) Maximal spiking frequency was also significantly elevated. CTR $n = 25$ cells, 7 organoids; CASPR2 $n = 45$ cells, 7 organoids. Each dot represents one cell. Data is presented as mean ± SEM. Statistical tests: Repeated measures two-way ANOVA (c) and two-tailed Mann–Whitney test in (d); significance: $^{**}p < 0.01$, $^{****}p < 0.0001$.

We then performed an analysis of long-square current injection protocols to assess if the changes in fAHP would influence neuronal excitability (Figure 3a,b). Here, we observed an increase in AP firing frequencies in CASPR2-Ab treated organoids along various levels of current injection (Main effect of treatment $F_{(68,1700)} = 13.93$, $p < 0.001$; Figure 3b,c). We also quantified the maximum average firing frequency between both conditions, which revealed a significantly higher maximal firing rate in neurons from CASPR2-Ab organoids (CTR = 2.00 ± 0.374 Hz, $n = 25$; CASPR2 = 4.67 ± 0.5605 Hz, $n = 45$; $p = 0.0013$). As expected, the observed hyperexcitability is consistent with impaired Kv1 channel function (Smart et al. 1998). Finally, to determine whether these alterations would translate into spontaneous neuronal hyperactivity, we monitored Ca^{2+} dynamics in acute organoid slices loaded with Fluo-4 AM (Figure 4a,b). Under this paradigm, CASPR2-exposed organoids displayed a significantly higher frequency of spontaneous Ca^{2+} transients compared with controls (CTR = 0.058 ± 0.0047 Hz, $n = 44$; CASPR2 = 0.096 ± 0.011 Hz, $n = 37$; $p = 0.0063$; Figure 4c,d). These findings further support the notion that CASPR2 antibodies promote neuronal hyperexcitability in 6-month-old organoids.

To determine whether the observed excitability defects arose from gross developmental alterations or specific defects in membrane properties, we performed qRT-PCR analysis across distinct cell lineages. We first evaluated neural stem cell and progenitor maintenance using SOX2 and PAX6, followed by TUJ1 to assess general neuronal differentiation. Subtype specification was characterized using SLC17A7 (VGLUT1) and SATB2 for excitatory populations, and GAD1 and DLX2 for inhibitory interneurons. While these major neuronal subtype markers remained stable between groups, we detected significant alterations in glial lineage markers, including the oligodendrocyte markers OLIG2 ($p < 0.01$) and SOX6 ($p = 0.0587$); nevertheless, we failed to amplify mature myelination genes (MAG, MAL or MOG) in both groups. We also detected increased expression of the astrocyte marker GFAP ($p < 0.001$). Given the absence of changes in neuronal specification, these glial alterations are consistent with an increase in neuronal activity acting as a driving force for enhanced glial maturation, oligodendrogenesis, and astrocyte differentiation (Gibson et al. 2014; Cohen and Fields 2008). Finally, we quantified the voltage-gated channels KCNA1 (Kv1.1), KCNA2 (Kv1.2), KCNC1 (Kv3.1), and SCN1A (Nav1.1) and observed no significant alterations. The lack of transcriptional changes in the expression of these channels further supports a mechanism stemming from functional defects in membrane mechanisms rather than altered expression profiles (Figure S4).

Together, our results demonstrate that long-term exposure of human brain organoids to CASPR2-Ab does not alter basic membrane properties or action potential initiation, but instead specifically enhances excitatory synaptic transmission and reduces the amplitude of the fAHP, consistent with impaired Kv1 channel function. This is further supported by the increased evoked firing rates and higher frequency of spontaneous Ca^{2+} transients. Collectively, these convergent findings establish that CASPR2 antibodies drive a state of neuronal hyperexcitability in 6-month-old organoids, providing mechanistic evidence for the pathogenic role of CASPR2 dysfunction in human brain development.

4 | Discussion

CASPR2 antibody-mediated diseases are associated with high levels of CASPR2 antibodies in the serum and/or cerebrospinal fluid. Patients with this condition can be afflicted by syndromes that include neuromyotonia, Morvan's syndrome, and

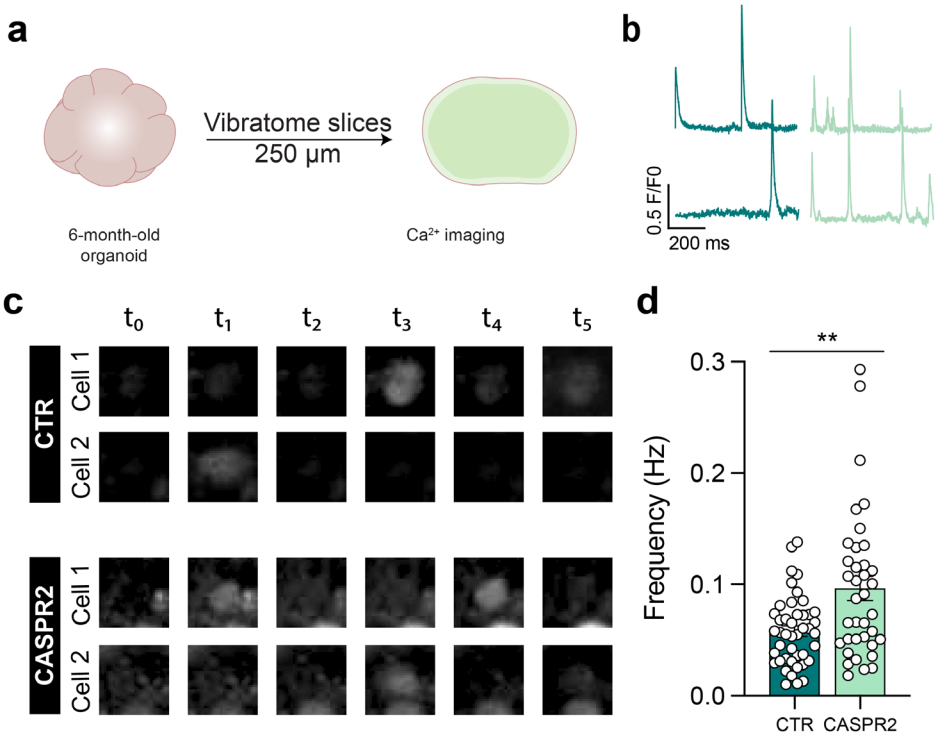

FIGURE 4 | Long-term incubation with CASPR2-Ab produces neuronal hyperexcitability. (a) Ca2+ imaging was performed in 250 µm acute slices from neural organoids. (b, c) Time course of live calcium imaging (b) from CTR and CASPR2 and exemplary ROIs (c). (d) Frequency of Ca^{2+} transients indicate increased neuronal activity in CASPR2-Ab exposed organoids. Each dot represents the average signal of a single ROI, which represents a local microdomain that may contain more than one single cell. CTR: $n = 44$; CASPR2-Ab: $n = 37$ ROIs. Two-tailed Mann–Whitney test. Data are presented as mean ± SEM. $^{**}p < 0.01$.

limbic encephalitis (Irani et al. 2010). In addition, CASPR2-Ab have been associated with neurodevelopmental disorders arising from gestational maternal transfer of antibodies to the fetus (Coutinho, Jacobson, et al. 2017; Brimberg et al. 2016). However, the alterations inflicted on neurophysiology and neuronal network activity during human brain development have not been studied. Here, using human brain organoids as a model, we show that human CASPR2 antibodies directly impact neuronal function and neuro development.

Our findings reveal that CASPR2-Ab do not grossly perturb intrinsic membrane properties or action potential initiation, but instead exert specific effects on synaptic connectivity and action potential repolarization. In terms of synaptic changes, a central observation was the increase in both the frequency and amplitude of sEPSCs in neurons from CASPR2-Ab exposed organoids. This enhancement of excitatory drive aligns with previous reports implicating CNTNAP2 in regulating glutamatergic synapse stability and dendritic spine development (Anderson et al. 2012; Fernandes et al. 2019; Varea et al. 2015). Such changes in synaptic strength and connectivity likely contribute to the increase in spontaneous Ca^{2+} transients observed during live recordings of acute organoid slices and provide a potential substrate for neuronal hyperexcitability. Importantly, these data extend rodent findings into a human-derived system, reinforcing the notion that CASPR2 dysfunction disrupts the balance between excitatory and inhibitory signaling.

At the level of action potential dynamics, we identified a selective reduction in the amplitude and depth of the fAHP, without major changes in spike threshold, amplitude, rise time, or decay time. Additionally, we found no significant alterations in cell capacitance, membrane resistance, resting membrane potential, or rheobase, which suggests that the observed perturbations in membrane properties are not the result of major or widespread alterations, but rather reflect discrete, localized alterations. These specific alterations point to dysfunction of Kv1 channels, which normally mediate the rapid repolarizing currents underlying the fAHP (Storm 1988; Smart et al. 1998). Given that CASPR2 associates with Contactin-2 to cluster Kv1 channels at juxtaparanodal domains (Poliak et al. 2003; Pinatel et al. 2017; Traka et al. 2003), the most parsimonious interpretation is therefore that antibody-mediated interference with CASPR2 destabilizes this complex, impairing Kv1 function. The resulting attenuation of fAHP predictably enhanced neuronal excitability, in agreement with our finding of elevated firing rates under prolonged current injection and the spontaneous activity obtained under calcium imaging. These findings are also in accordance with data in the literature showing that impaired CASPR2/Contactin-2 complex gives rise to alterations in VGKC response and neuronal hyperexcitability (Dawes et al. 2018; Fernández et al. 2021). In the present work, we also attempted to amplify myelin-associated genes but failed to do so. This is consistent with literature on unguided cerebral organoids, which consistently shows that although glial progenitors emerge around 5–6 months in vitro, the development of compact myelin is typically rare or entirely absent unless pro-myelinating factors, directed patterning, or co-culture strategies are introduced (Urrestizala-Arenaza et al. 2024). Therefore, while we observed the emergence of OLIG2 expression at 6 months, indicative of

oligodendrocyte precursor cells, we failed to find evidence of compact myelination. Consequently, the canonical clustering of CASPR2 and Kv1 at the juxtaparanodes is likely not yet established in this model. Regardless, CASPR2 and Kv1 critically cluster at the axon initial segment (Pinatel et al. 2017). As this region is the primary site for action potential initiation, this localization provides a mechanistic basis for our observations of altered neuronal excitability (specifically fAHP and firing frequency) in developing human circuits and likely preceding the formation of myelinated domains.

Importantly, neuronal hyperactivity can itself drive accelerated synaptic maturation and changes in postsynaptic properties; therefore, while the increased frequency in spontaneous synaptic events could be directly explained by the changes in overall network connectivity, the changes in the amplitude of these events may be interpreted as arising from modifications at the postsynaptic site. This could occur via: (i) a mechanism directly interfering with CASPR2 and glutamate receptors at the synapse (Anderson et al. 2012; Varea et al. 2015; Fernandes et al. 2019); or (ii) changes in synaptic physiology and synaptic maturation secondary to changes in neuronal activity (Zhang and Poo 2001; Katz and Shatz 1996); or (iii) a combination of both mechanisms. The potential for accelerated maturation of neuronal circuits may also be inferred from the increased proportion of neurons that fulfilled inclusion criteria, together with the higher probability of spiking across different stimulation paradigms in CASPR2-Ab exposed organoids, and even from the trend seen in increased cell capacitance (an indirect measure of neuronal complexity and size). These changes are then consistent with activity-dependent maturation processes, whereby enhanced neuronal excitability facilitates the recruitment of functional neurons into active circuits and promotes the refinement of synaptic connectivity (Zhang and Poo 2001; Katz and Shatz 1996). Additionally, our finding of increased expression of oligodendrocyte precursors and astrocyte markers in organoids exposed to CASPR2-Ab is also consistent with the notion that increased neuronal activity will influence the maturation of glial networks (Gibson et al. 2014; Cohen and Fields 2008).

Neuronal hyperexcitability may therefore be present as the key consequence from the pathological presence of CASPR2-Ab during early neurodevelopment, which points to early defects in excitation/inhibition ratio as an overarching underlying alteration in various ASDs (Rubenstein and Merzenich 2003; Manyukhina et al. 2022; Sohal and Rubenstein 2019). Moreover, the adult administration of human CASPR2 monoclonal Abs into mice was also sufficient to induce brain hyperexcitability as recorded by EEG and altered social behaviors in rodents (van Hoof et al. 2024), indicating a convergent phenotype of network hyperactivity that can arise from either early developmental perturbation or acute functional blockade of CASPR2 in the postnatal period. Interestingly, excitatory transmission was also found to be altered in *CNTNAP2* deletion models (Kim et al. 2019; Jurgensen and Castillo 2015; Vogt et al. 2018; Anderson et al. 2012; Lazaro et al. 2019; Lu et al. 2021). Moreover, in several studies, CASPR2 loss reduces GABAergic interneuron subpopulations, resulting in impaired GABAergic inhibitory transmission and increased excitability during postnatal development (Anderson et al. 2012; Bridi et al. 2017; Jurgensen and Castillo 2015; Lauber et al. 2018; Peñagarikano et al. 2011; Lu et al. 2021; Vogt et al. 2018). Additionally, during early development, in a *CNTNAP2* KO mouse cortical organoid model, deficits in inhibitory neurons were also observed, contributing to E/I imbalance (Hali et al. 2020). Interestingly, by restoring the E/I balance, a rescue of the hyperactivity phenotype was observed in models lacking *CNTNAP2* (Selimbeyoglu et al. 2017; Hali et al. 2020), demonstrating the importance of this gene for E/I ratio and network activity (Selimbeyoglu et al. 2017). However, we did not detect gross alterations in inhibitory neuron markers. It is likely that the stage of development analyzed was not sufficiently prolonged to assess consequences in mature inhibitory subtypes, which tend to arise later in development. For instance, PVALB interneurons show a characteristic protracted and postnatal maturation; consequently, their presence in organoid cultures is typically not observed at significant levels. Indeed, single-cell sequencing of organoids has demonstrated that while broad GABAergic markers (e.g., GAD, DLX) are detected, mature subclass markers (such as PVALB) are rare or absent in standard protocols (Pollen et al. 2015; Quadrato et al. 2017). Thus, a potential direct impact of CASPR2-Ab on mature inhibitory neuron activity must be addressed in future studies utilizing patterned organoids or longer developmental periods.

In conclusion, our data supports the view that in early human brain development models, the presence of CASPR2-Ab contributes to neuronal hyperexcitability, creating early markers for future E/I imbalance, even before the full maturation of the inhibitory system.

Author Contributions

Ana Rafaela Oliveira: investigation, conceptualization, methodology, writing – original draft, writing – review and editing, formal analysis, visualization. **Giuseppe Cammarata:** investigation, methodology, formal analysis. **Catarina Seabra:** conceptualization, methodology. **Ana Maria Cardoso:** investigation, methodology. **Henrique J. Santos:** investigation, methodology. **Joana Guedes:** methodology. **Diana Sequeira:** resources. **João Miguel Marques Santos:** resources. **Guiomar Oliveira:** resources. **Ana Luísa Cardoso:** resources, writing – review and editing. **Dominique Fernandes:** investigation, methodology, formal analysis. **Maria Isabel Leite:** resources. **Ester Coutinho:** resources. **Ana Luísa Carvalho:** methodology, formal analysis, investigation. **Lino Ferreira:** resources. **João Peça:** conceptualization, supervision, funding acquisition, project administration, resources, writing – original draft, writing – review and editing.

Acknowledgments

This research was funded by the European Union's Horizon 2020 research and innovation programme under grant agreement 799164 and 813986 and by the European Regional Development Fund (ERDF), through the Centro 2020/2030 (CENTRO2030-FEDER-02359000) and through the COMPETE 2020—Operational Programme for Competitiveness and Internationalization and Portuguese national funds via FCT—Fundação para a Ciência e a Tecnologia. J.P. and his group are supported by: PTDC/NEU-SCC/3247/2014; PTDC/MED-NEU/5993/2020; 2022.02604.PTDC; ERA-NET NEURON—FCT/NEURON/0002/2021; Bial Foundation (#427/2024) and institutional projects: UIDP/04539/2020, UIDB/04539/2020, and LA/P/0058/2020. The authors of this work were also funded by Programa Operacional Potencial Humano (POPH) through fellowships PD/BD/139074/2018 (to A.R.O.) and SFRH/BPD/120611/2016 (to J.G.) and by the European Union under the Horizon Research and Innovation Program (project

Syn2Psy, grant agreement no. 813986). Open access publication funding provided by FCT (b-on).

Funding

This work was supported by the European Union Horizon 2020 (799164, 813986), European Regional Development Fund (ERDF), Fundação para a Ciência e a Tecnologia (PTDC/NEU-SCC/3247/2014, PTDC/MED-NEU/5993/2020, 2022.02604.PTDC, FCT/NEURON/0002/2021), Bial Foundation (427/2024), CENTRO2030-FEDER-02359000, and Programa Operacional Potencial Humano (PD/BD/139074/2018, SFRH/BPD/120611/2016).

Conflicts of Interest

The authors declare no conflicts of interest.

Data Availability Statement

The authors declare that the data supporting the findings of this study are available within the paper and its Supporting Information files. The data, protocols and biological materials included in this study are available from the corresponding author upon reasonable request. Portions of the manuscript were included from the following thesis: "CASPR2 Autoimmune Antibodies Modify the Developmental Trajectory and Network Activity in Human Brain Organoids". Oliveira, Ana Rafaela Gomes Soares. Universidade NOVA de Lisboa (Portugal) ProQuest Dissertations & Theses, 2023, 31019200. https://www.proquest.com/docview/3059435240.

References

Alarcón, M., B. S. Abrahams, J. L. Stone, et al. 2008. "Linkage, Association, and Gene-expression Analyses Identify CNTNAP2 as an Autism-Susceptibility Gene." *American Journal of Human Genetics* 82: 150–159.

Anderson, G. R., T. Galfin, W. Xu, J. Aoto, R. C. Malenka, and T. C. Südhof. 2012. "Candidate Autism Gene Screen Identifies Critical Role for Cell-Adhesion Molecule CASPR2 in Dendritic Arborization and Spine Development." *Proceedings of the National Academy of Sciences of the United States of America* 109: 18120–18125.

Bagnall-Moreau, C., P. T. Huerta, D. Comoletti, et al. 2020. "In Utero Exposure to Endogenous Maternal Polyclonal Anti-Caspr2 Antibody Leads to Behavioral Abnormalities Resembling Autism Spectrum Disorder in Male Mice." *Scientific Reports* 10: 14446.

Bertil Hille, D. K. 1992. *Ionic Channels of Excitable Membranes*. Vol. 306. Second ed, 277–278. Sinauer Assoc. Inc.

Bridi, M. S., S. M. Park, and S. Huang. 2017. "Developmental Disruption of GABAAR-Meditated Inhibition in Cntnap2 KO Mice." *eNeuro* 4: ENEURO.0162-17.2017.

Brimberg, L., S. Mader, V. Jeganathan, et al. 2016. "Caspr2-Reactive Antibody Cloned From a Mother of an ASD Child Mediates an ASD-Like Phenotype in Mice." *Molecular Psychiatry* 21: 1663–1671.

Cohen, J. E., and R. D. Fields. 2008. "Activity-Dependent Neuron-Glial Signaling by ATP and Leukemia-Inhibitory Factor Promotes Hippocampal Glial Cell Development." *Neuron Glia Biology* 4: 43–55.

Coutinho, E., L. Jacobson, M. G. Pedersen, et al. 2017. "CASPR2 Autoantibodies Are Raised During Pregnancy in Mothers of Children With Mental Retardation and Disorders of Psychological Development but Not Autism." *Journal of Neurology, Neurosurgery, and Psychiatry* 88: 718–721.

Coutinho, E., D. A. Menassa, L. Jacobson, et al. 2017. "Persistent Microglial Activation and Synaptic Loss With Behavioral Abnormalities in Mouse Offspring Exposed to CASPR2-Antibodies In Utero." *Acta Neuropathologica* 134: 567–583.

Dawes, J. M., G. A. Weir, S. J. Middleton, et al. 2018. "Immune or Genetic-Mediated Disruption of CASPR2 Causes Pain Hypersensitivity due to Enhanced Primary Afferent Excitability." *Neuron* 97: 806–822.e10.

Fernandes, D., S. D. Santos, E. Coutinho, et al. 2019. "Disrupted AMPA Receptor Function Upon Genetic- or Antibody-Mediated Loss of Autism-Associated CASPR2." *Cerebral Cortex* 29: 4919–4931.

Fernández, M., C. A. Sánchez-León, J. Llorente, et al. 2021. "Altered Cerebellar Response to Somatosensory Stimuli in the Cntnap2 Mouse Model of Autism." *eNeuro* 8: ENEURO.0333-21.2021.

Gdalyahu, A., M. Lazaro, O. Penagarikano, P. Golshani, J. T. Trachtenberg, and D. H. Geschwind. 2015. "The Autism Related Protein Contactin-Associated Protein-Like 2 (CNTNAP2) Stabilizes New Spines: An In Vivo Mouse Study." *PLoS One* 10: e0125633.

Gibson, E. M., D. Purger, C. W. Mount, et al. 2014. "Neuronal Activity Promotes Oligodendrogenesis and Adaptive Myelination in the Mammalian Brain." *Science* 344: 1252304.

Guedes, J. R., P. A. Ferreira, J. Costa, et al. 2023. "IL-4 Shapes Microglia-Dependent Pruning of the Cerebellum During Postnatal Development." *Neuron* 111: 3435–3449.e8.

Hali, S., J. Kim, T. H. Kwak, H. Lee, C. Y. Shin, and D. W. Han. 2020. "Modelling Monogenic Autism Spectrum Disorder Using Mouse Cortical Organoids." *Biochemical and Biophysical Research Communications* 521: 164–171.

Howden, S. E., J. P. Maufort, B. M. Duffin, A. G. Elefanty, E. G. Stanley, and J. A. Thomson. 2015. "Simultaneous Reprogramming and Gene Correction of Patient Fibroblasts." *Stem Cell Reports* 5: 1109–1118.

Irani, S. R., S. Alexander, P. Waters, et al. 2010. "Antibodies to Kv1 Potassium Channel-Complex Proteins Leucine-Rich, Glioma Inactivated 1 Protein and Contactin-Associated Protein-2 in Limbic Encephalitis, Morvan's Syndrome and Acquired Neuromyotonia." *Brain: A Journal of Neurology* 133: 2734–2748.

Joubert, B., M. Petit-Pedrol, J. Planagumà, et al. 2022. "Human CASPR2 Antibodies Reversibly Alter Memory and the CASPR2 Protein Complex." *Annals of Neurology* 91: 801–813.

Jurgensen, S., and P. E. Castillo. 2015. "Selective Dysregulation of Hippocampal Inhibition in the Mouse Lacking Autism Candidate Gene CNTNAP2." *Journal of Neuroscience* 35: 14681–14687.

Katz, L. C., and C. J. Shatz. 1996. "Synaptic Activity and the Construction of Cortical Circuits." *Science* 274: 1133–1138.

Kim, J.-W., K. Park, R. J. Kang, et al. 2019. "Pharmacological Modulation of AMPA Receptor Rescues Social Impairments in Animal Models of Autism." *Neuropsychopharmacology: Official Publication of the American College of Neuropsychopharmacology* 44: 314–323.

Lancaster, E., M. G. M. Huijbers, V. Bar, et al. 2011. "Investigations of caspr2, an Autoantigen of Encephalitis and Neuromyotonia." *Annals of Neurology* 69: 303–311.

Lancaster, M. A., and J. A. Knoblich. 2014. "Generation of Cerebral Organoids From Human Pluripotent Stem Cells." *Nature Protocols* 9: 2329–2340.

Lancaster, M. A., M. Renner, C.-A. Martin, et al. 2013. "Cerebral Organoids Model Human Brain Development and Microcephaly." *Nature* 501: 373–379.

Lauber, E., F. Filice, and B. Schwaller. 2018. "Dysregulation of Parvalbumin Expression in the Cntnap2−/− Mouse Model of Autism Spectrum Disorder." *Frontiers in Molecular Neuroscience* 11: 262.

Lazaro, M. T., J. Taxidis, T. Shuman, et al. 2019. "Reduced Prefrontal Synaptic Connectivity and Disturbed Oscillatory Population Dynamics in the CNTNAP2 Model of Autism." *Cell Reports* 27: 2567–2578.e6.

Lu, P., F. Wang, S. Zhou, et al. 2021. "A Novel CNTNAP2 Mutation Results in Abnormal Neuronal E/I Balance." *Frontiers in Neurology* 12: 712773.

Manyukhina, V. O., A. O. Prokofyev, I. A. Galuta, et al. 2022. "Globally Elevated Excitation-Inhibition Ratio in Children With Autism Spectrum Disorder and Below-Average Intelligence." *Molecular Autism* 13: 20.

Martins, M., A. R. Oliveira, S. Martins, et al. 2023. "A Novel Genetic Variant in MBD5 Associated With Severe Epilepsy and Intellectual Disability: Potential Implications on Neural Primary Cilia." *International Journal of Molecular Sciences* 24: 12603.

Oliveira, A. R., S. Martins, G. Cammarata, et al. 2022. "Generation and Characterization of Novel iPSC Lines From a Portuguese Family Bearing Heterozygous and Homozygous GRN Mutations." *Biomedicine* 10: 1905.

Paşca, A. M., S. A. Sloan, L. E. Clarke, et al. 2015. "Functional Cortical Neurons and Astrocytes From Human Pluripotent Stem Cells in 3D Culture." *Nature Methods* 12: 671–678.

Peñagarikano, O., B. S. Abrahams, E. I. Herman, et al. 2011. "Absence of CNTNAP2 Leads to Epilepsy, Neuronal Migration Abnormalities, and Core Autism-Related Deficits." *Cell* 147: 235–246.

Pfaffl, M. W. 2001. "A New Mathematical Model for Relative Quantification in Real-Time RT-PCR." *Nucleic Acids Research* 29: e45.

Pinatel, D., B. Hivert, M. Saint-Martin, et al. 2017. "The Kv1-Associated Molecules TAG-1 and Caspr2 Are Selectively Targeted to the Axon Initial Segment in Hippocampal Neurons." *Journal of Cell Science* 130: 2209–2220.

Poliak, S., L. Gollan, R. Martinez, et al. 1999. "Caspr2, a New Member of the Neurexin Superfamily, Is Localized at the Juxtaparanodes of Myelinated Axons and Associates With K+ Channels." *Neuron* 24: 1037–1047.

Poliak, S., D. Salomon, H. Elhanany, et al. 2003. "Juxtaparanodal Clustering of Shaker-Like K+ Channels in Myelinated Axons Depends on Caspr2 and TAG-1." *Journal of Cell Biology* 162: 1149–1160.

Pollen, A. A., T. J. Nowakowski, J. Chen, et al. 2015. "Molecular Identity of Human Outer Radial Glia During Cortical Development." *Cell* 163: 55–67.

Quadrato, G., T. Nguyen, E. Z. Macosko, et al. 2017. "Cell Diversity and Network Dynamics in Photosensitive Human Brain Organoids." *Nature* 545: 48–53.

Renner, M., M. A. Lancaster, S. Bian, et al. 2017. "Self-Organized Developmental Patterning and Differentiation in Cerebral Organoids." *EMBO Journal* 36: 1316–1329.

Rodenas-Cuadrado, P., J. Ho, and S. C. Vernes. 2014. "Shining a Light on CNTNAP2: Complex Functions to Complex Disorders." *European Journal of Human Genetics* 22: 171–178.

Rubenstein, J. L. R., and M. M. Merzenich. 2003. "Model of Autism: Increased Ratio of Excitation/Inhibition in Key Neural Systems." *Genes, Brain and Behavior* 2: 255–267.

Selimbeyoglu, A., C. K. Kim, M. Inoue, et al. 2017. "Modulation of Prefrontal Cortex Excitation/Inhibition Balance Rescues Social Behavior in CNTNAP2-Deficient Mice." *Science Translational Medicine* 9: eaah6733.

Smart, S. L., V. Lopantsev, C. L. Zhang, et al. 1998. "Deletion of the KV1.1 Potassium Channel Causes Epilepsy in Mice." *Neuron* 20: 809–819.

Sohal, V. S., and J. L. R. Rubenstein. 2019. "Excitation-Inhibition Balance as a Framework for Investigating Mechanisms in Neuropsychiatric Disorders." *Molecular Psychiatry* 24: 1248–1257.

Storm, J. F. 1988. "Temporal Integration by a Slowly Inactivating K+ Current in Hippocampal Neurons." *Nature* 336: 379–381.

Strauss, K. A., E. G. Puffenberger, M. J. Huentelman, et al. 2006. "Recessive Symptomatic Focal Epilepsy and Mutant Contactin-Associated Protein-Like 2." *New England Journal of Medicine* 354: 1370–1377.

Tanaka, Y., B. Cakir, Y. Xiang, G. J. Sullivan, and I.-H. Park. 2020. "Synthetic Analyses of Single-Cell Transcriptomes From Multiple Brain Organoids and Fetal Brain." *Cell Reports* 30: 1682–1689.e3.

Traka, M., L. Goutebroze, N. Denisenko, et al. 2003. "Association of TAG-1 With Caspr2 Is Essential for the Molecular Organization of Juxtaparanodal Regions of Myelinated Fibers." *Journal of Cell Biology* 162: 1161–1172.

Urrestizala-Arenaza, N., S. Cerchio, F. Cavaliere, and C. Magliaro. 2024. "Limitations of Human Brain Organoids to Study Neurodegenerative Diseases: A Manual to Survive." *Frontiers in Cellular Neuroscience* 18: 1419526.

van Hoof, S., J. Kreye, C. Cordero-Gómez, et al. 2024. "Human Cerebrospinal Fluid Monoclonal CASPR2 Autoantibodies Induce Changes in Electrophysiology, Functional MRI, and Behavior in Rodent Models." *Brain, Behavior, and Immunity* 122: 266–278.

Varea, O., M. D. Martin-de-Saavedra, K. J. Kopeikina, et al. 2015. "Synaptic Abnormalities and Cytoplasmic Glutamate Receptor Aggregates in Contactin Associated Protein-Like 2/Caspr2 Knockout Neurons." *Proceedings of the National Academy of Sciences of the United States of America* 112: 6176–6181.

Vogt, D., K. K. A. Cho, S. M. Shelton, et al. 2018. "Mouse Cntnap2 and Human CNTNAP2 ASD Alleles Cell Autonomously Regulate PV+ Cortical Interneurons." *Cerebral Cortex* 28: 3868–3879.

Zhang, L. I., and M. M. Poo. 2001. "Electrical Activity and Development of Neural Circuits." *Nature Neuroscience* 4S: 1207–1214.

Supporting Information

Additional supporting information can be found online in the Supporting Information section. **Data S1:** jnc70388-sup-0001-DataS1.pdf.